Dissociation of van der Waals Complexes in High Rydberg States Induced by Electric Fields

Th. L. Grebner, P. v. Unold, and H. J. Neusser*

Institut für Physikalische und Theoretische Chemie, Technische Universität München, Lichtenbergstrasse 4, D-85748 Garching, Germany

Received: August 8, 1996; In Final Form: October 24, 1996[⊗]

Due to its mass and energy selectivity, mass-analyzed threshold ionization spectroscopy provides information on the energetic position of the dissociation threshold of van der Waals complex cations. In this work we report the first observation of a shift of the dissociation threshold of van der Waals complexes in high Rydberg states induced by an applied electric field of several hundred V/cm. The detection of a ≈70 cm^{-1} shift is possible for fluorobenzene·Ar because of its high density of optically accessible vibrational states around the dissociation threshold at 568 cm^{-1}. This shift is explained by a field-induced coupling between high and low Rydberg states of different series.

Introduction

The dissociation behavior of van der Waals (vdW) complexes of aromatic molecules has been subject of extensive theoretical and experimental investigations.[1−16] Because of their small binding energy, the ionization of vdW complexes by one- or two-photon ionization is often accompanied by a simultaneous fragmentation when the excess energy above the adiabatic ionization energy (AIE) exceeds the dissociation energy. For that reason it is important to control the amount of energy deposited in the complex ion by the excitation process. A powerful technique to precisely determine the internal energy of molecular and cluster ions is the mass-selective detection of threshold ions (mass-analyzed threshold ionization (MATI) spectroscopy[10,17,18]). This technique is based on the excitation of high long-lived Rydberg states and their subsequent ionization in a pulsed electric field. In addition to the ZEKE-PFI (zero kinetic energy electron spectroscopy by pulsed field ionization) technique[19] which monitors electrons after ionization of the Rydberg states, the MATI technique has the advantage of selective mass analysis and is thus able to detect any mass change of the ionic core after the excitation process.

In recent work we have shown that the dissociation of cluster ions can be monitored by the MATI technique as a function of its selected internal energy by a simultaneous observation of threshold ions at the complex ion mass and the fragment ion mass.[10,20] We were able to find upper values for the dissociation energy of van der Waals complexes of aromatic molecules like benzene and dibenzofuran with Ar and Kr atoms attached to the planar molecular surface.[20,21] Accurate values for the dissociation energy were obtained for the dibenzo-*p*-dioxin·Ar, dibenzo-*p*-dioxin·^{84}Kr,[16] and the fluorobenzene·Ar complex[22] because they have a large density of vibrational states in the excess energy range 500−900 cm^{-1} where dissociation takes place. Fluorobenzene represents a particularly suitable system for the state-selected observation of dissociation. Here the dissociation threshold is located several tens of cm^{-1} above an intramolecular vibrational state ($6b^1$) in an excess energy range which can be populated by excitation of additional low-frequency vdW (bending) modes. Thus, the system offers a dense series of 12 cm^{-1} accessible vibrational states in the region of the dissociation threshold.

In this work we report on experiments where the energetic position for the appearance of the dissociation product (daughter ions) is found to depend on the strength of the applied field leading to the field ionization of the earlier excited Rydberg states. This effect becomes visible in the present experiment because of (i) the vibrational state-selected preparation of the ionic core, (ii) the mass selectivity of the used detection technique, and (iii) the dense manifold of optically accessible vibrational states in the dissociation range. The last point is realized for vdW systems where dissociation thresholds are so low (≈500−800 cm^{-1}) that dissociation occurs in the Franck−Condon accessible energy range and where low-frequency intermolecular vibrations exist. The observed field-induced shift of the dissociation threshold is explained by a field-induced coupling of the originally excited high Rydberg states to lower Rydberg states of another series converging to higher vibrational states within the dissociation continuum of the ionic core. Coupling of high to lower Rydberg states is expected for many molecular systems but is difficult to detect in a ZEKE or a MATI experiment since bunches of Rydberg states are excited. In the present experiment this coupling is directly monitored by the resulting dissociation of the ionic core.

Experimental Section

The experimental setup used was described elsewhere.[16] Briefly, it consists of two dye lasers with ≈10 ns light pulses and ≈0.3 cm^{-1} bandwidth (FL 3002 and LPD 3000; Lambda Physik), which are pumped synchronously by an excimer laser (EMG 1003i, 308 nm; Lambda Physik). The two laser beams intersect perpendicularly a skimmed supersonic molecular beam. The pulses overlap in time and space in the ion optics of a linear reflecting time-of-flight mass spectrometer.[9] The supersonic jet is obtained by seeding the fluorobenzene vapor in Ar carrier gas at ≈3 bar backing pressure and expanding the mixture into the vacuum. The excitation of molecules or complexes to high Rydberg levels is achieved by a resonantly enhanced two-photon two-color process. Promptly produced cations originating from a one-color, a two-color two-photon ionization process, or a prompt ionization of molecules excited to Rydberg levels are separated from the molecules in long-lived high Rydberg states by a delayed pulsed electric field (separation field, ≈0.6 V/cm), which is applied to the first zone (30 mm wide), in a way that the prompt ions are decelerated. The separation field is switched

[⊗] Abstract published in *Advance ACS Abstracts,* December 15, 1996.

S1089-5639(96)02419-X CCC: $14.00

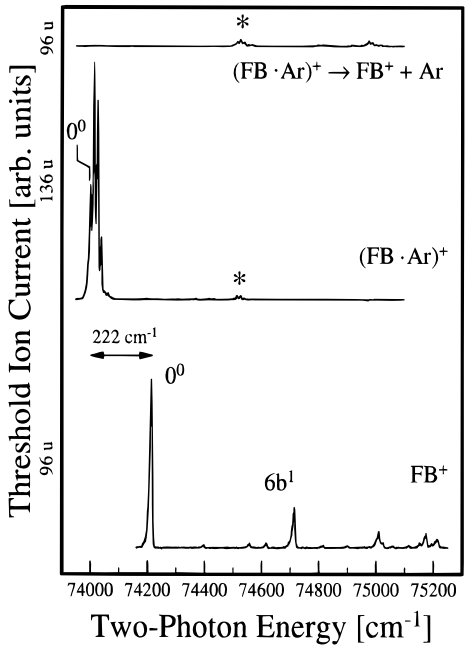

Figure 1. Threshold ion spectrum of fluorobenzene (bottom) and fluorobenzene·Ar measured at mass 96 u (middle) and 136 u (top). The adiabatic ionization energy (AIE, 0^0) of the van der Waals complex at 74 000 cm^{-1} is red-shifted by -222 cm^{-1} from the AIE of the bare molecule at 74 222 cm^{-1}. Note the small peak at 74 500 cm^{-1} marked by asterisks appearing in the upper two spectra. For explanation, see text.

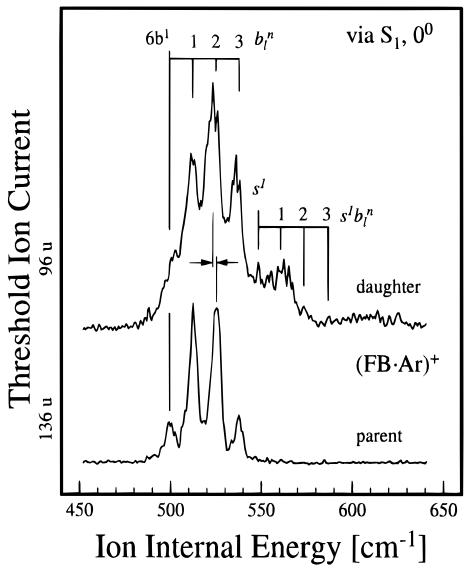

Figure 2. Lower trace: threshold ion spectrum of fluorobenzene·Ar between 450 and 650 cm^{-1} ion internal energy after excitation via the S_1, 0^0 intermediate state. Upper trace: same excitation conditions, however, threshold ion current simultaneously measured at the daughter ion (96 u), (fluorobenzene)$^+$ mass. The spectra are displayed on the same intensity scale.

on ≈100 ns after the occurrence of the two laser pulses.[23] After several microseconds the high Rydberg molecules reach the second zone (20 mm wide) where no electric field is present at that time. Pulsed field ionization of the high Rydberg molecules and acceleration of the produced threshold ions toward the reflector are achieved by a pulsed electric field (ionization field) which is varied between 125 and 975 V/cm. The ionization field is delayed by 30−50 μs with respect to the two exciting/ionizing laser pulses. Threshold ion spectra are recorded mass selectively by a gated integrator/microcomputer system.

Results

Threshold Ion Spectra. Using the technique described above, a threshold ion spectrum of bare fluorobenzene (FB, 96 u) was recorded by resonance-enhanced two-photon excitation via the S_1, 0^0 intermediate state. It is shown in Figure 1 (bottom). The most prominent peak at the lowest two-photon energy of 74 222 cm^{-1} corresponds to the adiabatic ionization energy (AIE, 0^0) of FB.[22] We assigned the peak at +500 cm^{-1} ion internal energy to the $6b^1$ mode, which was found at +519 cm^{-1} in the S_1 intermediate state.[24] The threshold ion spectrum of the van der Waals complex FB·Ar (136 u) is shown in the middle trace in Figure 1. It was measured with the frequency of the first laser fixed to the S_1, 0_0^0 transition. The origin of the complex threshold ion spectrum is located at 74 000 cm^{-1} and shifted by -222 cm^{-1} to the red of the bare molecule origin. The origin band of the complex cation shows additional vibrational structure arising from the excitation of vdW modes. In recent work we assigned the vibration leading to the progression as the long in-plane bending mode b_l.[22] Different from the bare molecule spectrum, only a weak feature appears at an ion internal energy of about +500 cm^{-1} in the complex threshold ion spectrum (see the asterisk in Figure 1, middle trace). The spectrum on top of Figure 1 represents the daughter ion spectrum (FB^+, 96 u) which was recorded simultaneously with the threshold ion spectrum of (FB·Ar)$^+$ (middle trace, 136 u) for the same excitation conditions but with the mass gate set to 96 u. No peaks are detected in the energy region of the AIE, but weak structures are found for ion internal energies exceeding 500 cm^{-1} (asterisk).

A magnified part of the threshold parent ion spectrum measured at the parent mass of (FB·Ar)$^+$ (Figure 1, middle) and the simultaneously recorded spectrum measured at the mass of the charged dissociation product FB^+ (Figure 1, top) are shown in the lower and the upper trace of Figure 2, respectively. It displays the weak features on a magnified scale which are present around 500 cm^{-1} ion internal energy and marked by asterisks in Figure 1. (Note that in the following text we denote complex threshold ion spectra recorded at the parent mass channel "parent spectra" and complex spectra recorded at the mass channel of the charged dissociation product "daughter spectra".)

Both spectra show a progression of vibrational bands with a distance of ≈12 cm^{-1} starting at 500 cm^{-1}. The progression is attributed to the long in-plane bending mode b_l similar to the progression observed at the electronic origin of the ionic complex. The vibrational origin at 500 cm^{-1} corresponds to the $6b^1$ vibration found at 500 cm^{-1} in the bare molecule ion, indicating a small frequency shift of this vibrational mode after complexation with Ar.[22] Note the slight red shift of the peaks in the daughter spectrum compared to the parent spectrum as indicated in Figure 2 by the two horizontal arrows.

In Figure 3 the threshold ion spectrum of (FB·Ar)$^+$ measured at the parent mass (parent spectrum) and obtained by pumping via the first quantum of the vdW stretching mode (S_1, 0^0s^1) in the intermediate state is shown in an energy range from 460 to 660 cm^{-1} (lower trace). The upper trace represents the simultaneously recorded daughter spectrum. In the parent spectrum the transitions to the $6b^1$ vibrational mode, to the $6b^1s^1$, and to the $6b^1s^1b_l^1$ combination states are visible. All progression members with $n > 1$ of the b_l^n progression are missing in the parent spectrum (lower trace) but are present up to $n = 3$ in the daughter spectrum (upper trace). The signal in the parent spectrum breaks down at 568 cm^{-1} just below the $6b^1s^1b_l^2$ vibrational progression located at 573 cm^{-1}. At higher ion

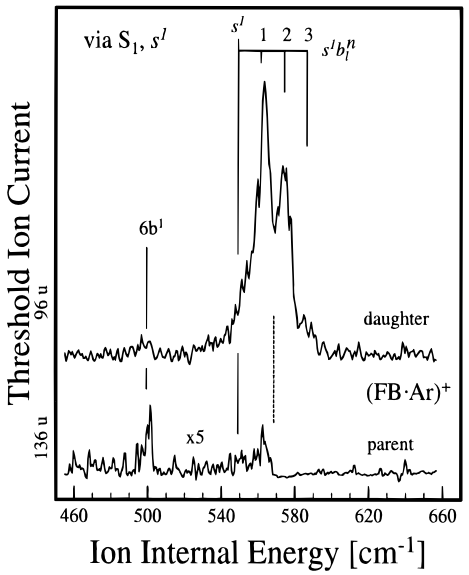

Figure 3. Lower trace: threshold ion spectrum of fluorobenzene·Ar between 460 and 660 cm^{-1} ion internal energy after excitation via the S_1, 0^0s^1 intermediate state. Upper trace: same excitation conditions; however, threshold ion current simultaneously measured at the daughter ion, $(fluorobenzene)^+$ mass. The broken line at 568 cm^{-1} indicates the position of the dissociation threshold of the complex (see text). Note that the intensity scale in the lower trace is magnified by a factor of 5.

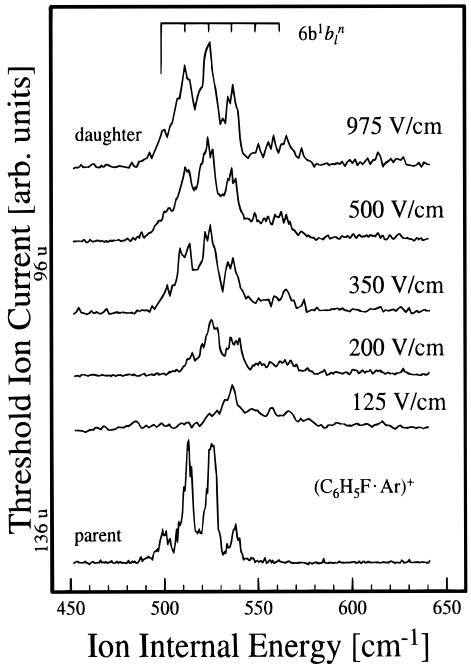

Figure 4. Upper five traces: threshold ion spectra of fluorobenzene·Ar measured at the $fluorobenzene^+$ daughter mass between 450 and 650 cm^{-1} ion internal energy after excitation via the S_1, 0^0 intermediate state with five different ionization field strengths from 125 to 975 V/cm. Lower trace: threshold ion spectrum of fluorobenzene·Ar measured at the parent mass with 500 V/cm ionization field strength. The spectra are displayed on the same intensity scale.

internal energies no transitions are visible in the parent spectrum, but some appear in the daughter spectrum. This indicates that practically all van der Waals complex ions have dissociated above 568 cm^{-1} internal energy.

As a result of the experimental findings, three different energy regions of the complex ion spectra can be distinguished: (i) 0−490 cm^{-1} ion internal energy: The 0^0 peak is only observed in the parent spectrum. No signal appears in the daughter spectra since no dissociation of the complex cation takes place (see Figure 1). (ii) 490−568 cm^{-1} internal energy: Transitions are observed in the parent spectrum as well as in the daughter spectrum. In this energy range some of the complex ions remain intact and others dissociate (Figures 1 and 2). (iii) Ion internal energies >568 cm^{-1} (indicated by the broken line in Figure 2): No signal is observed for ion internal energies in excess of 568 cm^{-1} in the parent spectrum. On the other hand, the daughter spectrum continues up to an excess energy of ≈590 cm^{-1}.

Electric Field Effect. Next we measured parent and daughter spectra in the energy region from 450 to 650 cm^{-1} ion internal energy with a different strength of the ionization and acceleration field which is applied 46 μs after the laser pulses. The intermediate state selected was the same as for the spectra shown in Figure 2 (S_1, 0^0). In these experiments the slew rate of the ionization field is not constant but varies by a factor of 3 at 5.4 V cm^{-1} ns^{-1} (125 V/cm pulse), 6.7 V cm^{-1} ns^{-1} (200 V/cm pulse), 12.5 V cm^{-1} ns^{-1} (350 V/cm pulse), 16.8 V cm^{-1} ns^{-1} (500 V/cm pulse), and 11.9 V cm^{-1} ns^{-1} (975 V/cm pulse). In Figure 4 five threshold ion spectra recorded at the daughter mass (daughter spectrum) with decreasing field strength are displayed (975−125 V/cm, from top to bottom) and one parent spectrum obtained with 500 V/cm field strength (bottom). Only one parent spectrum is shown since all parent spectra recorded simultaneously with each daughter spectrum look essentially the same. This demonstrates that no experimental artifacts are responsible for the changes in the daughter spectra, and all other experimental parameters remained constant throughout this series of experiments. All spectra were recorded with the same sensitivity.

The upper three daughter spectra are quite similar: No significant difference is observed for 975, 500, and 350 V/cm ionization field strength. For 200 V/cm the lowest transition leading to the $6b^1$ vibration at 500 cm^{-1} ion internal energy is not visible, and the first member of the progression produced by the long in-plane bending progression at ≈513 cm^{-1} has nearly disappeared. For 125 V/cm field strength even the second member of the bending progression disappears and the first band observed is the $6b^1s^1b_l^3$ band. This series of daughter spectra clearly indicates that the threshold for appearance of signal in the daughter spectra depends on the strength of the pulsed ionization field between 125 and 350 V/cm. Furthermore, a closer inspection reveals that similar to the finding in Figure 2 all peaks in the daughter spectra display a small red shift of ≈2.5 cm^{-1} from the respective peaks in the parent spectra and are slightly broader.

Discussion

Coupling Scheme. The striking experimental result presented in this work is the simultaneous appearance of threshold ion signal at the parent $(FB·Ar)^+$ and the daughter $(FB)^+$ ion mass within an internal energy range of ≈70 cm^{-1} for ionization fields larger than 350 V/cm (see Figures 2 and 3). This is similar to the finding in our recent work on dibenzo-*p*-dioxin·Ar where we observed an overlap region of both spectra between 717 and 731 cm^{-1} excess energy.[16] In this work we demonstrate that the width of the overlap region depends on the ionization field (see Figure 4) with a blue shift of its low-energy edge for decreasing ionization field. As a consequence, the onset of dissociation of the complex when taken as the appearance of threshold ions at the daughter mass (FB^+) appears to be shifted to lower energies for an increasing ionization field.

In this paragraph we discuss the origin of this shift and demonstrate that we are able to use the data to deduce an accurate value for the field-free dissociation threshold of the

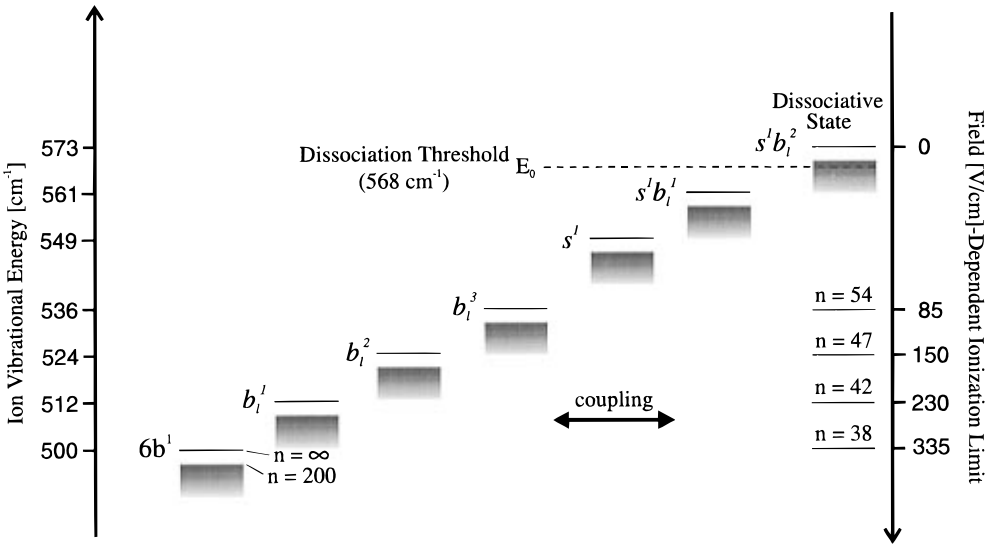

Figure 5. Scheme of the coupling between Rydberg states of different vibrational states in $(FB{\cdot}Ar)^+$ from 500 to 573 cm^{-1} ion internal energy (left scale). The long-lived high Rydberg states $n > 150$ (left side) are coupled to lower Rydberg levels $n \approx 40$ (right side), converging to a dissociative vibrational state ($6b^1s^1b_l^2$) above the ionic dissociation energy E_0. The low Rydberg levels can be ionized by the electric field indicated on the right scale.

complex cation. The lowering of the dissociation threshold of the ionic core due to a distortion of the potentials as observed in refs 25 and 26 is too small for the weak electric fields used in our experiments. Therfore, any dissociation below the true (field-free) dissociation threshold requires a transfer of electronic energy of the Rydberg electron to the vibrational degrees of freedom of the complex ion core. This can be induced by a coupling of Rydberg series converging to different vibrational states of the complex ion core. Nonradiative decay of high Rydberg states in polyatomic molecules has been discussed by several authors.[27−29] Here we have to include the possibility of a dissociation, because this decay channel is open in a weakly bound van der Waals complex when we excite the core close to the dissociation threshold so that a small amount of additional energy transfered to the core leads to its rapid dissociation. We performed RRKM calculations with a phase space limited to the vdW motions[2,9] yielding a fast dissociation rate of 10^9 s^{-1} at threshold. Let us consider the situation where a high long-lived ($n \geq 150$) Rydberg state of a series converging to a vibrational state of the ion core *below* the dissociation threshold (e.g., the $6b^1$ state in Figure 5) is excited. If no coupling to a lower lying Rydberg state exists, no dissociation would be observed and a signal exclusively at the parent ion mass be monitored. If, on the other hand, the excited high Rydberg state is coupled to a lower n Rydberg state of a series converging to a vibrational state *above* the dissociation threshold, the complex ion core dissociates even though the original ion internal energy deposited by the optical excitation is smaller than the dissociation energy. Dissociation can be detected if the ionizing field strength is sufficient to ionize the low Rydberg state. The coupling scheme is schematically shown in Figure 5. Let us consider, for example, the $n = 150$ Rydberg state of the $6b^1$ vibrational state which is coupled to a $n \approx 38$ Rydberg state of the $6b^1s^1b_l^2$ level *above* the dissociation threshold E_0. As a result of this coupling, electronic energy is converted to vibrational energy, leading to a dissociation of the complex cation core. For the Rydberg electron this coupling results in a change of the n quantum number to lower values, and consequently higher pulsed fields are needed for ionization of these lower Rydberg states. If dissociation of the complex is very fast, it is assumed that the high Rydberg orbit survives the dissociation of the ionic core. Experimental evidence for fast dissociation with stable Rydberg orbits has been found in our recent work.[20]

The classical treatment of the diabatic lowering of the ionization limit ΔE by the ionization field F yields ΔE [cm^{-1}] $= \alpha\sqrt{F[V/cm]}$ with a predominant value for α of ≈ 4.[30] This leads to $\Delta E = 125$ cm^{-1} for 975 V/cm, $\Delta E = 89$ cm^{-1} for 500 V/cm, $\Delta E = 75$ cm^{-1} for 350 V/cm, $\Delta E = 56$ cm^{-1} for 200 V/cm, and $\Delta E = 44$ cm^{-1} for 125 V/cm for the five ionization fields used in our experiments.

For an ionization field in excess of 350 V/cm all Rydberg states within ≈ 75 cm^{-1} ($n \geq 38$) below the ionization threshold can be ionized. In FB·Ar six optical accessible vibrational states (see Figure 5) are located down to 75 cm^{-1} below the dissociation threshold, which is found at 568 cm^{-1} (see below). This special situation is due to the fact that (i) the dissociation threshold is located close to an optical active intramolecular vibration, (ii) the density of van der Waals vibrations is very high because of their low frequency, and (iii) these vdW vibrations are accessible by suitable Franck−Condon factors.[22] As a consequence, we can check directly which state is coupled by stepwise increase of the electric field from the lowest experimentally possible value of 125 V/cm to 350 V/cm. The lowest vibrational state which can be monitored in this way is the $6b^1$ state with no vdW vibration excited. Since the $6b^1$ vibrational state is located at 500 cm^{-1} ion internal energy and therefore less than 73 cm^{-1} below the dissociative state at ≈ 573 cm^{-1} ($6b^1s^1b_l^2$),no difference in each pair of parent and daughter spectra is expected and indeed observed for an ionization field exceeding 350 V/cm. This is due to the fact that no optically accessible state is located below the $6b^1$ state, which could become visible in the daughter spectrum. For 200 V/cm the lowering of the ionization threshold is 56 cm^{-1}, and therefore transitions in the daughter spectrum should be missing between 500 and 514 cm^{-1} since the Rydberg levels belonging to this energy region can no longer be ionized. This is in line with the observation that the transition to the $6b^1$ vibrational state and first member of the progression $6b^1b_l^1$ at ≈ 512 cm^{-1} has nearly disappeared in the corresponding spectrum of Figure 4. In case of 125 V/cm the lowering of the ionization threshold is 44 cm^{-1}, and therefore ionization can only occur for Rydberg states with $n > 53$ (down to 529 cm^{-1} below the ionization

limit). Again, this treatment is in line with the experimental observation that the second member of the bending progression $6b^1b_l^2$ at 524 cm^{-1} has disappeared in the daughter spectrum and the first transition observed corresponds to the $6b^1b_l^3$ band at 536 cm^{-1}.

Coupling Mechanism. By observation of the cluster dissociation, we found direct evidence for a coupling process between Rydberg series. Now the question arises whether the coupling to lower Rydberg states of the dissociative vibrational state is an intrinsic coupling of Rydberg series converging to different ionic vibrational states or is induced by electric fields present in the experiment (separation field and ionization field). To address this question, we have to consider the lifetime of the coupled low ($n \approx 38$) Rydberg states[27,30] which is not affected by the dissociation of the vdW core as mentioned above.[20] Do they survive the long delay of 46 μs between excitation and pulsed field ionization? There are two arguments against this: (i) The typical width of a threshold ion peak corresponding to a single vibrational state is on the order of less than 10 cm^{-1} (see e.g. Figure 2) with a separation field of 0.6 V/cm and an ionization field of 500 V/cm which is able to ionize Rydberg states down to 89 cm^{-1} ($n \approx 38$) below the ionization threshold. This means that Rydberg states with $n <$ 100 do not contribute to the MATI signal since most of them do not survive the long delay time. (ii) Recent line width measurements in the $n \approx 20$ range of bis(benzene)chromium point to subnanosecond lifetimes,[31] and decay time measurements of resolved $n = 45$ Rydberg states in benzene display a multiexponential decay behavior with a dominating short time component of less than 100 ns.[32]

Since the coupled low-n Rydberg states have lifetimes shorter than the delay time of 46 μs for ionization, we can exclude that the coupling exists already during excitation since a negligible fraction of Rydberg states of the dissociation product would have survived the delay until ionization occurs. This means that if the coupling would be significant under field-free conditions or during the presence of the separation field (0.6 V/cm), no signal would be present in the daughter spectrum for the case of the coupled low-n states. For this reason we conclude that the coupling is induced by the strong delayed ionization field providing the ionization. This conclusion is corroborated by the observation of a slight red shift of 2.5 cm^{-1} of the peaks in the daughter spectra. This red shift shows that the highest originally excited n states are not involved in the coupling process since their ionization by the strong field is more effective than the dissociation process. In a time-dependent picture we can compare the ionization rate with the Rydberg nonradiative relaxation rate of the vdW complex. Since ionization rates are field-dependent[33] competition between ionization and nonradiative relaxation followed by dissociation can occur during the rise time of the ionizing field pulse. Furthermore, red and blue Stark states behave in a different manner, e.g., the blue Stark states require a higher field for the same ionization rate, which might cause a higher dissociation probability for the complexes in blue Stark states.

Dissociation Energy. We have seen that the threshold for appearance of signal in the daughter spectra depends on the strength of the ionization field. Furthermore, we have developed a coupling scheme to explain this result. To find the true (field-free) dissociation threshold from the daughter spectra, we have to either correct for the field effect or investigate the parent spectra for complete disappearance of signal. If we take the lowest energetic appearance of signal in the lower three daughter spectra of Figure 4 and plot the ion internal energy as a function of square root of the ionization field, the experimental points

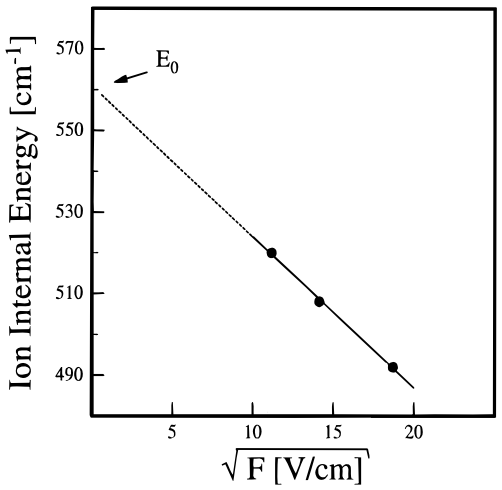

Figure 6. Ion internal energy determined from the appearance threshold in the lower three daughter spectra of Figure 4 as a function of square root of the strength F of the ionization field. The dotted line represents the linear extrapolation of the square root field dependence leading to the field-free dissociation threshold of $E_0 = 561$ cm^{-1} of the complex core.

can be fitted by a straight line. The extrapolation of this line to zero field leads to the field-free dissociation threshold of ≈561 cm^{-1} of the complex cationic core (Figure 6). This result is corroborated by the cutoff of the signal in the parent spectrum indicated by the dashed line (lower trace in Figure 3). From this figure we find a dissociation energy $E_0 = 568$ cm^{-1} in the ionic ground state of the FB·Ar vdW complex, which is in excellent agreement with the value determined by the extrapolation discussed above.

The accuracy of E_0 is governed by the 12 cm^{-1} spacing of the progressions of the long in-plane bending mode b_l and the relative accuracy of the ion internal energy scale which is estimated to be better than 1 cm^{-1}. From the red shift (ΔAIE $= -222$ cm^{-1}) of the AIE in the vdW complex, from that of the bare FB substrate we find the dissociation energy of the neutral complex in its ground state by $D_0 = E_0 - (AIE_{FB} - AIE_{FB\cdot Ar}) = 346 \pm 10$ cm^{-1}. The accuracy of this value is given by the accuracy of E_0 and of ΔAIE. This value agrees with the dissociation energy of benzene·Ar found with the MATI technique[20] and corroborated by a recent ab initio calculation.[34]

Summary and Conclusion

In this work we presented vibrational spectra of the $(fluorobenzene\cdot Ar)^+$ complex which have been obtained with the technique of mass-analyzed threshold ionization (MATI) spectroscopy. Due to its mass and internal energy selectivity, this technique allows the detection of the threshold for dissociation of weakly bound van der Waals complexes by the appearance of signal in the threshold ion spectrum of the van der Waals complex measured at the daughter mass. In $(FB\cdot Ar)^+$ a series of closely lying vibrational states are located in the energy region of the dissociation threshold so that the internal energy of the complex cation can be varied in steps of 12 cm^{-1} between 500 and 573 cm^{-1} internal energy. As a new result, we found that the dissociation threshold determined in this way is dependent on the strength of the electric field applied 46 μs after laser excitation to field ionize the highly excited Rydberg states. It varies from 492 to 508 to 520 cm^{-1} for electric fields of 350, 200, and 125 V/cm, respectively. From the measured square root field dependence of the dissociation threshold the field-free value was determined.

The finding is important for the interpretation of ion spectra recorded by MATI spectroscopy especially if dissociation

processes are examined. We explain the field effect by a field-induced coupling mechanism between the high $n \approx 150$ Rydberg states optically excited and lower Rydberg states of another series converging to a vibrational state above the dissociation threshold. This coupling is induced by the delayed ionization field and can finally lead to the dissociation of the complex. As a possible mechanism of the field-induced coupling, we propose the Stark splitting of the Rydberg states involved in the coupling process which may lead to a closer resonance of the coupled states. In conclusion, the field-induced dissociation process enables one to detect coupling between different Rydberg series monitored on a mass different from that of the originally excited species. Van der Waals complexes turn out to be suitable systems as they provide a dense manifold of vibrational states which facilitate the achievement of resonance conditions of Rydberg states in different series and make the coupling more likely.

Acknowledgment. We thank R. Neuhauser for helpful discussions. Financial support from the Deutsche Forschungsgemeinschaft and the Fonds der Chemischen Industrie is gratefully acknowledged.

References and Notes

(1) Beswick, J. A.; Jortner, J. *Adv. Chem. Phys.* **1981**, *47*, 363.
(2) Kelley, D. F.; Bernstein, E. R. *J. Phys. Chem.* **1986**, *90*, 5164.
(3) Ewing, G. E. *J. Phys. Chem.* **1987**, *91*, 4662.
(4) Brumbaugh, D. V.; Kenny, J. E.; Levy, D. H. *J. Chem. Phys.* **1983**, *78*, 3415.
(5) Stephenson, T. A.; Rice, S. A. *J. Chem. Phys.* **1984**, *81*, 1083.
(6) Butz, K. W.; Catlett Jr, D. L.; Ewing, G. E.; Krajnovich, D.; Parmenter, C. S. *J. Phys. Chem.* **1986**, *90*, 3533.
(7) Knee, J. L.; Khundkar, L. R.; Zewail, A. H. *J. Chem. Phys.* **1987**, *87*, 115.
(8) Easter, D. C.; El-Shall, M. S.; Hahn, M. Y.; Whetten, R. L. *Chem. Phys. Lett.* **1989**, *157*, 277.
(9) Ernstberger, B.; Krause, H.; Kiermeier, A.; Neusser, H. J. *J. Chem. Phys.* **1990**, *92*, 5285.
(10) Krause, H.; Neusser, H. J. *J. Chem. Phys.* **1992**, *97*, 5923.
(11) Nakai, Y.; Ohashi, K.; Nishi, N. *J. Phys. Chem.* **1992**, *96*, 7873.
(12) Beck, S. M.; Hecht, J. H. *J. Chem. Phys.* **1992**, *96*, 1975.
(13) Neusser, H. J.; Krause, H. *Int. J. Mass Spectrom. Ion Processes* **1994**, *131*, 211.
(14) Droz, T.; Bürgi, T.; Leutwyler, S. *J. Chem. Phys.* **1995**, *103*, 4035.
(15) Cheng, B.-M.; Grover, J. R.; Walters, E. A. *Chem. Phys. Lett.* **1995**, *232*, 364.
(16) Th.L. Grebner, H. J. Neusser, *Chem. Phys. Lett.* **1995**, *245*, 578.
(17) Zhu, L.; Johnson, P. M. *J. Chem. Phys.* **1991**, *94*, 5769.
(18) Jouvet, C.; Dedonder-Lardeux, C.; Martrenchard-Barra, S.; Solgadi, D. *Chem. Phys. Lett.* **1992**, *198*, 419.
(19) Reiser, G.; Habenicht, W.; Müller-Dethlefs, K.; Schlag, E. W. *Chem. Phys. Lett.* **1988**, *152*, 119.
(20) Krause, H.; Neusser, H. J. *J. Chem. Phys.* **1993**, *99*, 6278.
(21) Grebner, Th.L.; Stumpf, R.; Neusser, H. J. Submitted to *Int. J. Mass Spectrom. Ion Processes*.
(22) Grebner, Th.L.; Neusser, H. J. *Int. J. Mass Spectrom. Ion Processes*, in press.
(23) Dietrich, H. J.; Lindner, R.; Müller-Dethlefs, K. *J. Chem. Phys.* **1994**, *101*, 3399.
(24) Lipp, E. D.; Seliskar, C. J. *J. Mol. Spectrosc.* **1981**, *87*, 242.
(25) Bjerre, N.; Keiding, S. R. *Phys. Rev. Lett.* **1986**, *56*, 1459.
(26) Carrington, A.; McNab, I. R.; Montgomerie, C. *Chem. Phys. Lett.* **1988**, *151*, 258.
(27) Chupka, W. A. *J. Chem. Phys.* **1993**, *99*, 5800.
(28) Remacle, F.; Levine, R. D. *J. Chem. Phys.* **1996**, *104*, 1399.
(29) Bixon, M.; Jortner, J. *J. Phys. Chem.* **1995**, *99*, 7466.
(30) Chupka, W. A. *J. Chem. Phys.* **1993**, *98*, 4520.
(31) Even, U.; Levine, R. D.; Bersohn, R. *J. Phys. Chem.* **1994**, *98*, 3472.
(32) Neuhauser, R.; Neusser, H. J. *Chem. Phys. Lett.* **1996**, *253*, 151.
(33) Gallagher, Th. F. *Rydberg Atoms*, Cambridge Monographs, 1994.
(34) Kraka, E.; Cremer, D.; Spoerel, U.; Merke, I.; Stahl, W.; Dreizler, H. *J. Phys. Chem.* **1995**, *99*, 12466.